Available online at www.sciencedirect.com
ScienceDirect
Ceramics International 34 (2008) 1539–1542
CERAMICS INTERNATIONAL
www.elsevier.com/locate/ceramint

Agglomeration of α-Al_2O_3 powders prepared by gel combustion

Jiang Li [a,b], Yusong Wu [a,b], Yubai Pan [a,*], Wenbin Liu [a], Yong Zhu [a,b], Jingkun Guo [a]

[a] State Key Lab of High Performance Ceramics and Superfine Microstructures, Shanghai Institute of Ceramics,
Chinese Academy of Sciences, Shanghai 200050, PR China
[b] Graduate School of the Chinese Academy of Sciences, Beijing 100039, PR China

Received 2 January 2007; received in revised form 5 March 2007; accepted 27 April 2007
Available online 20 July 2007

Abstract

Ultrafine α-Al_2O_3 powders were prepared by a gel combustion method and the agglomeration characteristic of the resultant powders was studied. A variety of fine crystallite α-Al_2O_3 powders with different agglomeration structures could be obtained by altering the citrate-to-nitrate ratio γ and calcining the precursors at 1050 °C for 2 h. All the powders were of nearly equivalent crystallite size (60–80 nm) except for the P1 powder (113 nm) from the gel with $\gamma = 0.033$. The primary crystallites of the obtained α-Al_2O_3 powders were formed into large secondary particles with different degree of agglomeration. Except for the powder P1, the mean particle sizes from specific surface area and particle size distribution measurement increase with increasing citrate-to-nitrate ratio in the fuel-lean condition and decrease in the fuel-rich condition. Densities of alumina ceramics from powders P4 and P5 sintered at different temperatures were relatively low due to the wide particle size distribution.

Keywords: Agglomeration; α-Al_2O_3; Gel combustion

1. Introduction

Ultrafine α-Al_2O_3 is one of the most important ceramic powders with high melting point, high temperature stability, high chemical inactivity and high hardness. Its mechanical, electrical and optical properties enable a wide range of uses in many areas such as microelectronics, catalysis, refractories, optics and lasers. Combustion synthesis [1–6] is particularly a simple, safe and rapid production process, which can be used to synthesize high-purity, crystalline oxide ceramic powders including ultrafine alumina powders with a broad range of particle sizes. Ultrafine α-Al_2O_3 synthesized by combustion method was investigated using different chemicals such as urea [7], glycine [8,9] and citric acid [10] as fuel. The combustion process using citric acid, which is widely known as amorphous citrate process, is a much less exothermic reaction.

Recently, we have reported the preparation of ultrafine α-Al_2O_3 by the gel combustion method at lower temperature using aluminum nitrate and citric acid as raw materials. The decomposition of the citrate precursor, the transition and the morphology of alumina powder and the influence of citrate to nitrate ratio on the thermal behavior and chemical environment of alumina gel were investigated in our previous work [11–13]. In the present paper, the agglomeration characteristic of alumina powders prepared by gel combustion method was investigated.

2. Experimental

Analytical grade $Al(NO_3)_3{\cdot}9H_2O$ and citric acid ($C_6H_8O_7{\cdot}H_2O$) were dissolved in deionized water, and the citrate-to-nitrate ratio γ ($\gamma = M_{\mathrm{citrate}}/M_{\mathrm{nitrate}}$, M is the molar amount of the compound) was varied from 0.033 to 0.667. It can be calculated [1] that 0.833 mol of citric acid is required for each mol of nitrate in order to have a stoichiometric redox reaction in the gel that gives $\gamma = 0.278$ (named GS). Deficient citric acid in the gel with $\gamma = 0.033$, 0.1 and 0.167 (named G1, G2 and G3, respectively) presents a fuel-lean condition while higher citric acid concentration with $\gamma = 0.333$, 0.5 and 0.667 (named G4, G5 and G6, respectively) produce a fuel-rich condition. The mixed citrate–nitrate aqueous solution was continuously stirred and concentrated by evaporation at ~80 °C, producing a transparent gel. The gel was rapidly heated to 200 °C and then calcined at different temperatures

---

* Corresponding author. Tel.: +86 21 52412820; fax: +86 21 52413903.
E-mail address: ybpan@mail.sic.ac.cn (Y. Pan).

0272-8842/$34.00 © 2007 Elsevier Ltd and Techna Group S.r.l. All rights reserved.
doi:10.1016/j.ceramint.2007.04.022

for 2 h. The "powder" refers to the calcined product of the combusted ash. Gel and powder samples are named G# and P#, respectively. The prepared α-Al_2O_3 powders were mixed with 1.0 wt.% magnesium aluminosilicate (MAS) glass (17.5 wt.% MgO, 21.0 wt.% Al_2O_3 and 61.5 wt.% SiO_2), which was used as sintering aid. All the powder mixtures were dispersed in ethanol and ball milled with high-purity alumina balls for 24 h in corundum containers. After drying, the powders were screened through a 200-mesh sieve, uniaxially pressed into Ø20 mm disks under a pressure of 100 MPa and then cold isostatically pressed under 400 MPa. The sintering was conducted in air with a heating rate of 5 °C/min and a dwelling time of 3 h at the maximum temperature.

Phase identification was performed in a Rigaku D/max2200PC X-ray diffractometer (XRD) using nickel filtered Cu Kα radiation in the range of $2\theta = 10–80^\circ$ with a scanning speed of $4^\circ\ \mathrm{min}^{-1}$. Specific surface area analyses were conducted at 77 K using a Norcross ASAP 2010 Micromeritics, with N_2 as the absorbate gas. Samples were degassed at 150 °C until the air pressure was below 5×10^{-3} mmHg. The specific surface areas were calculated using the BET multipoint method with eight data points. Microstructures were observed on a JEOL JEM 2100F FETEM instrument. Samples were prepared using a carbon-coated copper grid (150 mesh). Powders were dispersed in ethanol using an ultrasonic horn, and then a drop of the dispersed powder/ethanol mixture was deposited on the grid. The grid was then dried in air. The FETEM was used with an accelerating voltage of 200 kV. The agglomeration particle size distribution was measured by a dynamic laser scattering (DLS) method on a Brookhaven ZetaPlus Zeta Potential Analyzer. The bulk densities of the sintered samples were measured by the Archimedes method.

3. Results and discussion

Fig. 1 shows XRD patterns of the 1050 °C calcined powders from gels with different citrate-to-nitrate ratios, which indicates that all the powders had crystallized completely. There was no evidence of any crystalline phase other than α-Al_2O_3. Crystallite size of the 1050 °C calcined powders was determined by the X-ray line broadening and calculated using the Scherrer equation:

$$d_{Crys} = \frac{0.89\lambda}{B\cos\theta}$$

where $B = (B_o^2 - B_c^2)^{1/2}$, B_o is the full width at half maximum (in 2θ (°)), B_c the correction factor for instrument broadening, θ the angle of the peak maximum (in 2θ (°)), and λ is the Cu Kα weighted average wavelength. The values of crystallite size calculated from the (0 1 2) XRD peak ($2\theta = 25.56^\circ$) are shown in Table 1. It could be seen that all the d_{XRD} values of powders were nearly equivalent except for that of P1. This was because the citrate-to-nitrate ratio γ of the gel played an important role in controlling the thermal behavior of the synthesized gel and it is only the gel G1 that decomposed in a single step, as mentioned in our previous work [13].

Table 1
Particle size of α-Al_2O_3 powders calcined at 1050 °C for 2 h

	Powder no.						
	P1	P2	P3	PS	P4	P5	P6
d_{XRD} (nm)	113	63	81	64	75	66	74
d_{BET} (nm)	331	308	312	318	306	231	164
d_{50} (nm)	416	679	887	628	573	494	322

Fig. 2 shows the surface areas of the 1050 °C calcined α-Al_2O_3 powders from gels with different citrate-to-nitrate ratios, respectively. Powder P1 has the lowest surface area because a complete combustion in a single step occurs in the case of gel G1 and the large crystallite size is the main factor to affect the specific surface area. For powders P2, P3 and PS, the corresponding gels decomposed in two steps. It can be seen in Fig. 2 that, for P2, P3 and PS, the surface area of the calcined powders slightly decreases with increasing the citrate-to-nitrate ratio. In the fuel-rich condition, the 200 °C calcined ash was not completely combusted. The decomposed gases from the remained carboxylate increased with γ and gases escaping through the initially forming crystalltes caused formation of a more porous network in the sample. Thus, for P4, P5 and P6, the surface area of the calcined powders increases as γ goes up. The particle average size is derived from the formula below. It may be assumed that with d_{BET} being the average particle size, ρ the

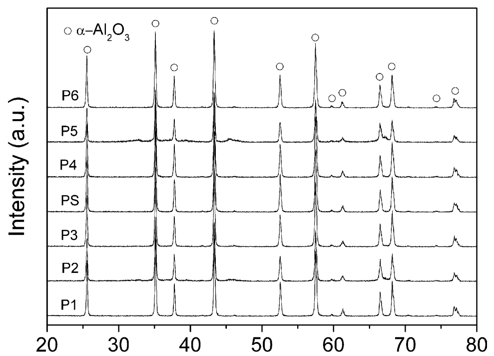

Fig. 1. XRD patterns of the powders calcined at 1050 °C for 2 h: P1; P2; P3; PS; P4; P5; P6.

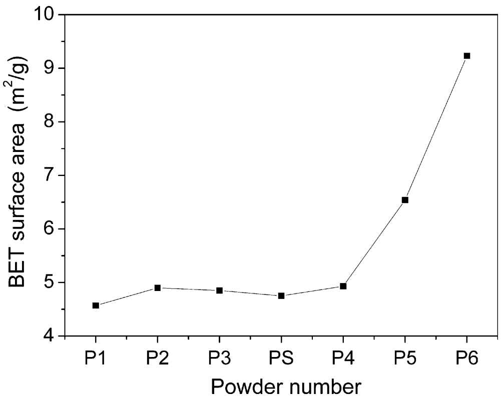

Fig. 2. BET surface areas of the powders calcined at 1050 °C for 2 h.

density of the material, and S_{ssa} its specific surface area.

$$d_{BET}=\frac{6}{\rho S_{ssa}}$$

Particle size obtained using the above formula is also given in Table 1. All the measured values of d_{BET} larger than d_{XRD} imply that nitrogen gas, used for BET measurement, can not completely cover the crystallite surfaces. Namely, it indicates the structure of agglomerate particles with the degree of connection of primary crystallites.

Fig. 3 shows the FETEM micrographs of the 1050 °C calcined α-Al_2O_3 powders from gels with different citrate-to-nitrate ratios of 0.167 (G2), 0.278 (GS), 0.5 (G5) and 0.667 (G6), respectively. It can be seen that the primary crystallites were fine, but they were formed into large secondary particles. Among the four powders, the primary crystallites of PS are relatively homogeneous and fine, ~108 nm in diameter.

The mean agglomerate size d_{50} was the median diameter determined from the particle size distribution measured by dynamic laser scattering (DLS) method. The particle size distributions of α-Al_2O_3 powders calcined at 1050 °C for 2 h are shown in Fig. 4. The values of the size d_{50} are summarized in Table 1. The mean secondary particle size increases with increasing the citrate-to-nitrate ratio in the fuel-lean condition and decreases in the fuel-rich condition. In comparison with the PS, P4 and P5 powders, the agglomerate particles of P1, P2, P3

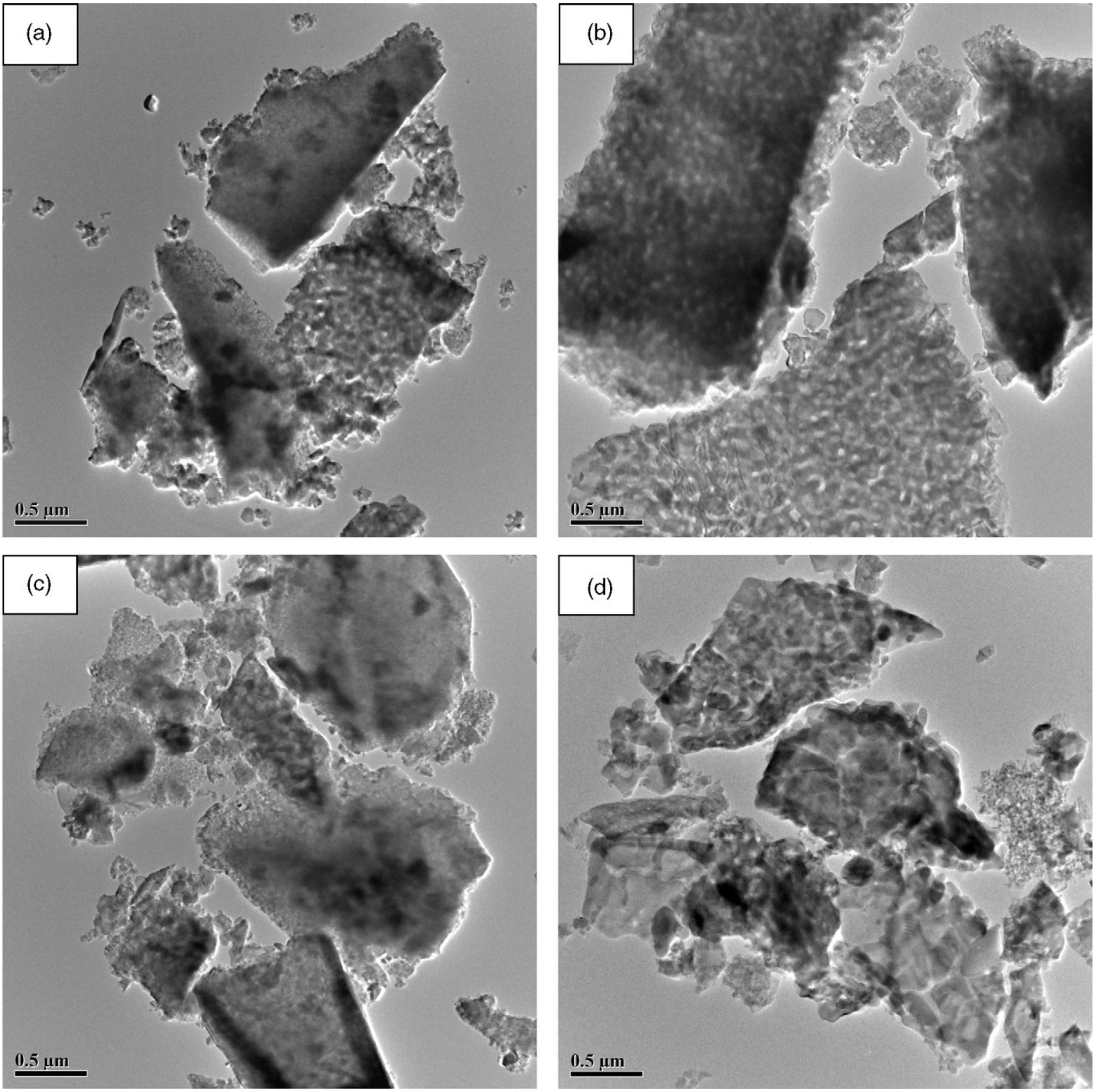

Fig. 3. FETEM micrographs of α-Al_2O_3 powders calcined at 1050 °C for 2 h: (a) P2; (b) PS; (c) P5; (d) P6.

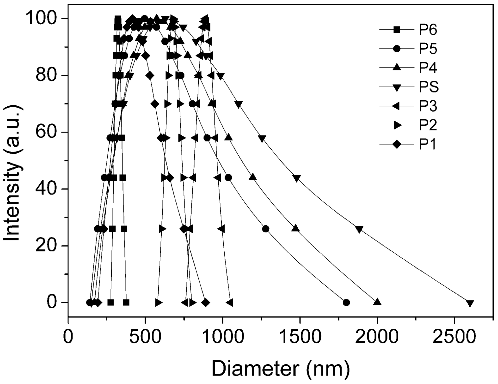

Fig. 4. Particle size distributions of α-Al_2O_3 powders calcined at 1050 °C for 2 h.

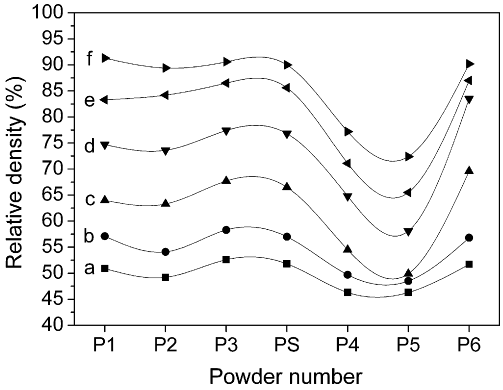

Fig. 5. Relative densities of alumina ceramics sintered at: (a) 1350 °C; (b) 1400 °C; (c) 1450 °C; (d) 1500 °C; (e) 1550 °C; (f) 1600 °C for 3 h.

and P6 powders prepared by the present method were found to be fine with a narrow size distribution.

Relative densities of alumina ceramics from α-Al_2O_3 powders P1, P2, P3, PS, P4, P5 and P6 sintered at different temperatures are shown in Fig. 5. It can be seen that density of the sample increases with increasing sintering temperature. Compared with P1, P2, P3, PS and P6, densities of alumina ceramics from powders P4 and P5 were relatively low due to the wide particle size distribution. Though the powder PS is of the widest secondary particle size distribution, the primary crystallites of PS are relatively homogeneous and fine. So the samples from powder PS are of the similar densities compared with those from powders P1, P2, P3 and P6.

4. Conclusions

A variety of α-Al_2O_3 powders with different agglomeration structures were obtained by altering the citrate-to-nitrate ratio γ and calcining the precursors at 1050 °C. All the powders were of nearly equivalent crystallite size except for the powder P1. The primary crystallites of the obtained α-Al_2O_3 powders were fine, but they were formed into large secondary particles. The mean secondary particle size increases with increasing the citrate-to-nitrate ratio in the fuel-lean condition and decreases in the fuel-rich condition. The powders PS, P4 and P5 have a relatively wide secondary particle size distribution. So, densities of alumina ceramics obtained by sintering of powders P4 and P5 are the lowest. However, the samples from powder PS are of the similar density as those from powders P1, P2, P3 and P6 due to the relatively homogeneous and fine primary crystallites.

Acknowledgements

This work was supported by the Applied Basic Research Programs of Science and Technology Commission Foundation of Shanghai (Grant No. 06DZ11417 and 05DZ22005) and the Key Project of Science and Technology of Shanghai (Grant No. 04DZ14002).

References

[1] S.S. Manoharan, K.C. Patil, Combustion synthesis of metal chromite powders, J. Am. Ceram. Soc. 75 (4) (1992) 1012–1015.

[2] S. Roy, W. Sigmund, F. Aldinger, Nanstructured yttria powders via gel combustion, J. Mater. Res. 14 (4) (1999) 1524–1531.

[3] S. Roy, A. Das Sharma, S.N. Roy, H.S. Maiti, Synthesis of $YBa_2Cu_3O_{7-x}$ powder by autoignition of citrate–nitrate gel, J. Mater. Res. 8 (11) (1993) 2761–2766.

[4] A. Chakrabort, P.S. Devi, S. Roy, H.S. Maiti, Low-temperature synthesis of ultrafine $La_{0.84}Sr_{0.16}MnO_3$ powder by an autoignition process, J. Mater. Res. 9 (4) (1994) 986–991.

[5] J. Li, Y.B. Pan, F.G. Qiu, Y.S. Wu, W.B. Liu, J.K. Guo, Synthesis of nanosized Nd:YAG powders via gel combustion, Ceram. Int. 33 (6) (2007) 1047–1052.

[6] J. Li, Y.B. Pan, F.G. Qiu, Y.S. Wu, J.K. Guo, Nanostructured Nd:YAG powders via gel combustion: the influence of citrate to nitrate ratio, Ceram. Int. 34 (1) (2008) 141–146.

[7] S. Bhaduri, E. Zhou, S.B. Bhaduri, Auto ignition processing of nanocrystalline α-Al_2O_3, Nanostruct. Mater. 7 (5) (1996) 487–496.

[8] J.C. Toniolo, M.D. Lima, A.S. Takimi, C.P. Bergmann, Synthesis of alumina powders by the glycine-nitrate combustion process, Mater. Res. Bull. 40 (3) (2005) 561–571.

[9] T.Y. Peng, X. Liu, K. Dai, J.R. Xiao, H.B. Song, Effect of acidity on the glycine-nitrate combustion synthesis of nanocrystalline alumina powder, Mater. Res. Bull. 41 (2006) 1638–1645.

[10] L.C. Pathak, T.B. Singh, S. Das, A.K. Verma, P. Ramachandrarao, Effect of pH on the combustion of nano-crystalline alumina powder, Mater. Lett. 57 (2002) 380–385.

[11] J. Li, Y.B. Pan, C.S. Xiang, Q.M. Ge, J.K. Guo, Low temperature synthesis of ultrafine α-Al_2O_3 powder by a simple aqueous sol–gel process, Ceram. Int. 32 (5) (2006) 587–591.

[12] J. Li, Y.S. Wu, Y.B. Pan, J.K. Guo, Alumina precursors produced by gel combustion, Ceram. Int. 33 (3) (2007) 361–363.

[13] J. Li, Y.S. Wu, Y.B. Pan, J.K. Guo, Influence of citrate to nitrate ratio on the thermal behavior and chemical environment of alumina gel, Ceram. Int. 33 (5) (2007) 735–738.